A.A. Nikolaeva[1,2], L.A. Konopko[1,2], P.P. Bodiul[1], A.K. Tsurkan[1]

[1]D. Gitsu Institute of Electronic Engineering and Nanotechnologies of the Academy of Sciences of Moldova, 3/3, Academiei Str., Kishinev, MD-2028, Republic of Moldova;
[2]International Laboratory of High Magnetic Fields and Low Temperatures, 95, Gajowicka Str., Wroclaw, 53-421, Poland

PECULIARITIES OF DIFFUSION THERMOPOWER WITH IMPURITY ELECTRON TOPOLOGICAL TRANSITION IN HEAVILY DOPED BISMUTH WIRES

This paper presents a series of investigations of differential thermopower and resistance in the temperature range of 4.2 – 300 K of samples shaped as glass-coated single-crystal Bi wires heavily doped with Sn acceptor impurity. An anomaly in the form of a triple sign change in the temperature dependences of thermopower $\alpha(T)$ is detected. The effect is treated in terms of impurity electron topological transition (ETT), i.e. origination of Σ-band by doping bismuth wires with Sn acceptor impurity. The method of measuring Shubnikov-de-Haas oscillations in the main crystallographic directions in parallel ($H \parallel I$) and perpendicular ($H \perp I$) directions was used to calculate the basic parameters of hole Fermi surfaces at points T and L of the Brillouin zone, which made it possible to estimate the concentration and energy position of Σ-band in Bi and confirm that anomalies observed on traditional dependences of diffusion thermopower are specific features of ETT. The effect can be used for the discovery of ETT in the cases when research on the Fermi surface by oscillation methods is impossible, for instance, with heavy doping and in high-temperature region.

Key words: electronic topological transitions, Shubnikov-de-Haas oscillations, diffusion thermopower, doped bismuth wires.

Introduction

Knowledge of the Fermi surface shape allows determination of many thermodynamic and kinetic characteristics of solids.

The kinetic and thermodynamic characteristics of solids are largely determined by the Fermi surface (FS) shape, since current carriers located in the Fermi layer are nearest to unoccupied states owing to which they are most efficient.

On application of various extreme external influences, namely introduction of isovalent and doping impurities, uniform compression and uniaxial deformations, etc., the Fermi surface can vary not only quantitatively, shrinking or expanding, but also qualitatively. Then the topology of this surface becomes radically different. Qualitative changes in the topology of the Fermi surface can result from change in the composition, for instance, at doping, and with constant composition, for instance, under pressure.

The density of energy states $\nu(\varepsilon) = dN(E)/dE$ of conduction electrons is due to the shape of constant-energy surfaces in momentum space $E(p) = E$. As was demonstrated by Lifshitz [1], the root peculiarity in the density of energy states of conduction electrons $\nu(E) = dN/dE$, occurring at certain

critical values of energy $E = E_k$, whereby FS topology is changed results in the appearance at low temperatures of anomaly in the series of thermodynamic and kinetic characteristics of metals.

In the majority of metals the value of critical energy E_k, where changes of FS topology take place is located sufficiently far from electron chemical potential μ, and the presence of particular points E_k can be judged by *X*-ray spectra. However, if there is any ever changing parameter with a change of which the difference (μ-E_k) passes through zero, i.e. the topology of the boundary Fermi surface is changed, then the peculiarities of spectral density $\nu(E)$ and the dynamics of electrons close to "critical" surface $E(p) = E_k$ lead to peculiar anomalies of thermodynamic and kinetic characteristics of electron gas in metal. Such a continuous parameter can be the level of doping with donor or acceptor impurities.

In [2], using pseudopotential method, calculations were performed for ETT of the type "formation of cavity" and "formation of jumper" in the system of $Li_{1-x}Mg_x$ alloys. It was emphasized that at critical point E_k, alongside with the root peculiarity in the density of states $\nu(E)$, there is a similar peculiarity of electron mean free path *l*. According to [3], this peculiarity occurs in relaxation time τ, so when considering the anomalies of kinetic characteristics, it is necessary to speak of relaxation time, rather than of electron mean free path peculiarities.

Various kinetic coefficients, in particular, electric conductivity σ_e and thermal conductivity χ, are equal to integrals of vector mean free path length $\vec{l}(\vec{p})$ along FS with different weight functions, hence, all of them comprise a peculiarity of the form $(\pm Z)^{1/2}\Theta(\pm Z)$, where $\Theta(Z) = 0$ at $Z < 0$ and $\Theta(Z) = 1$ at $Z > 0$.

Taking into account the expression for the electron part of thermopower α_e [4]:

$$\alpha_e = \frac{\pi^2 T}{3e} \cdot \frac{\partial \ln \sigma_e(E)}{\partial E}\Big|_{E=E_F} \tag{1}$$

the authors of [2, 5] were the first to point to the fact that the anomaly in α_e should be most strongly pronounced:

$$\alpha_e \sim (\pm Z)^{-1/2} \cdot \Theta(\pm Z) \tag{2}$$

At $Z \to 0$ the thermopower at point of ETT is very much increased, and this growth is restricted only by transition blurring.

The characteristic energies of *Bi* are very small. Having small characteristic energies, *Bi* is a representative of substances whose energy spectrum is extremely sensitive to various external influences, namely magnetic field, uniform compression, uniaxial deformations, introduction of doping and isovalent impurities. With the aid of external influences, one can realize in *Bi* various unique cases of mutual arrangement of *L* and *T* bands relative to each other and to the boundary filling energy.

For the bulk samples of *Bi* and $Bi_{1-x}Sb_x$ with impurities, in [6] it was shown that in conformity with theory the kinetic characteristics, namely resistance and thermopower, show an abnormal behaviour at ETT, the anomaly of thermopower, shaped as asymmetric peak, being particularly pronounced. All-round investigation of the anomalies of thermopower and resistance at ETT of all possible types was reliably recorded by means of Shubnikov-de-Haas (SdH) quantum oscillations. It was of interest to study the peculiarities of diffusion thermopower at ETT in *Bi* wires heavily doped with acceptor impurities with a view to discover heavy Σ-band.

Samples, experiment

Thin single-crystal wires were obtained by liquid phase casting by the Ulitovsky method [7, 8].

When casting thin wires of bismuth and its alloys, a single-crystal ingot prepared by zone re-crystallization method served as a source material.

To obtain *Sn*-doped *Bi* wires, the alloys of *Bi*-0.3 at.%, 0.07 and 0.05 at. % *Sn* were synthesized. The wires with concentrations of 0.1 at%, 0.15 at% and 0.2 at% *Sn* were obtained by dilution of alloys comprising 0.3 at% *Sn*. For this purpose, a glass tube with a sealed bottom was filled with several grams of *Bi*-0.3 at% *Sn* alloy, to which pure bismuth was added in estimated quantity necessary for obtaining the required concentration of donor impurity.

Crystallization of microwire strand of bismuth and its alloys occurs with strong overcooling of melt on crystallization front. Thus, for instance, for bismuth, maximum overcooling depth appears at casting rate 10 m/sec and achieves 40 – 50 °C. Strong overcooling and high crystallization rates contribute to growth of single-crystal strand.

Wire diameter $d > 1$ μm was measured by optical microscope Biolam with magnification 1350, as well as calculated by the resistance value at room temperature and the respective resistivity obtained for thicker samples according to expression: $d = \sqrt{\frac{4l}{\pi R_{300}\sigma_{300}}}$, where l is sample length, σ_{300} is conductivity of thick ($d > 1$ μm) wire of corresponding composition of this crystalloghraphic orientation at 300 K, R is sample resistance at 300 K. The error in diameter determination by the calculated method was ≈ 5 – 10 %.

Control diameter measurements were made on scanning electron microscope Vega Tescan 5130 MM.

Test measurements of crystallographic orientation of glass-coated wires were performed with the use of *X*-ray diffraction method. *X*-ray diffraction was performed in diffractometer Xcalibur of company Oxford Diffraction. Diffraction pattern showed that in the area of glass-coated wire illumination (*X*-ray beam diameter 0.5 mm) the nanowire is single-crystal. The instrument permitted to determine orientation of crystal crystallographic planes relative to its external faceting, which made it possible to determine lattice parameters and prove that direction (001) coincides with the wire axis (Fig. 1, insert).

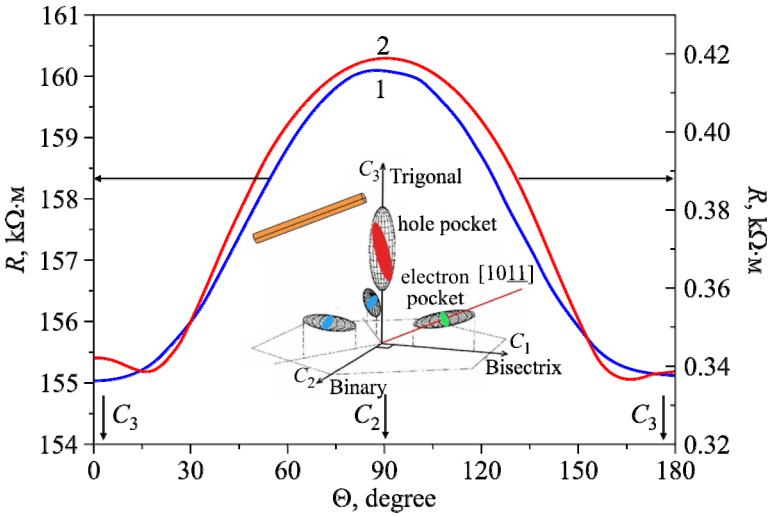

Fig. 1. Diagram of revolution of transverse magnetoresistance of Bi wires doped with Sn: 1. Bi – 0.05at.% Sn, d = 0.6 μ, 2. Bi – 0.1 at.% Sn, d = 1.5 μ, B = 0.5 T, T = 4.2 K. Insert: Schematic of bismuth Fermi surface with respect to wire axis.

Investigations of angular diagrams of revolution of the transverse magnetoresistance (Fig. 1) have confirmed the crystallographic orientation of wires under study, and permitted to orient wire-shaped samples in a magnetic field in such a way that vector $\vec{B}$ coincides with the principal crystallographic axes of the sample. Then Shubnikov-de-Haas oscillations were investigated in the respective direction. At θ = 0 (Fig. 1) magnetic field B is directed along axis C_3, and at θ = 90°, B || along the binary axis C_2.

Measurements were performed in the temperature range of 1.5 – 300 K. Studies of magneto-resistance $R(B)$ and derivative $\delta R/\delta H(B)$ in magnetic fields up to 14 T at temperatures 1.5 – 4.2 K were performed in the International Laboratory of High Magnetic Fields and Low Temperatures, Wroclaw, Poland.

Results and discussion

This paper studies the longitudinal and transverse magnetoresistance and SdH effect in a series of samples shaped as *Bi* wires doped with donor impurity of tin ≥ 0.3 at% *Sn*.

Fig. 2 shows the field dependences of longitudinal magnetoresistance (B || I) at 4.2 K of *Bi* wires with different degree of doping with *Sn*.

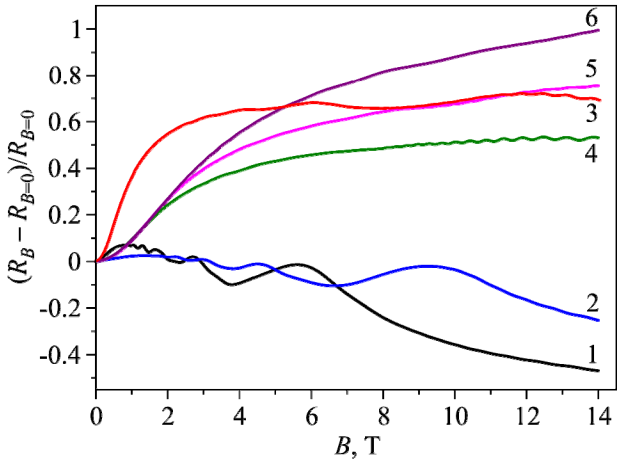

Fig. 2. Field dependences of reduced longitudinal magnetoresistance ΔR/R(B) (B || I) at T = 2.1 K of Bi-Sn wires of various composition: 1. Bi – 0.05 at% Sn, d = 0.6μm; 2. Bi – 0.07 at% Sn, d = 0.6 μm; 3. Bi – 0.1 at% Sn, d = 1.5 μm; 4. Bi – 0.15 at% Sn, d = 0.4 μm; 5. Bi – 0.2 at% Sn, d = 0.2 μm; 6. Bi – 0.3 at% Sn, d = 1.7 μm.

Monotone curves of longitudinal magnetoresistance $\Delta R/R(B)$ are essentially dependent on doping degree. In the wires *Bi* – 0.05 at% *Sn* and *Bi* – 0.07 at% *Sn* one can see the effect of negative magnetoresistance, when wire diameter is less than 1 μm (curves 1, 2, Fig. 2). The presence of negative magnetoresistance in combination with maximum formation on $R(B)$ in weak magnetic fields is primarily due to manifestation of galvanomagnetic size effect discovered earlier in thin wires of pure *Bi* and in *Bi-Sn* alloys with *Sn* concentration up to 0.025 at% [8, 9].

With further doping of N > 0.07 at% *Sn,* the effect of negative magnetoresistance disappears and is not manifested even at diameters 200 nm (curve 5, Fig. 1).

In heavily doped $Bi_{1-x}Sn_x$ wires in the area of weak magnetic fields there is a quadratic growth of resistance followed by saturation area in high magnetic fields up to 14 T with achievement of weak linear growth only in the wires with maximum degree of doping with *Sn* – 0.3 at% (curve 6, Fig. 2).

In all the wires investigated in a longitudinal magnetic field there were registered Shubnikov oscillations due to charge carriers at points *L* and *T* of reduced Brillouin zone in the range of magnetic fields up to 14 T and temperature range of $2.1 < T < 4.2$ K. In the wires *Bi* – 0.05 at% *Sn* and *Bi* – 0.07 at% *Sn* on *R*(*B*), just as on *dR*/*dB*(*B*) (Fig. 3) the amplitude of SdH oscillations due to light *L* holes in weak magnetic fields is sufficiently high even on *R*(*B*), despite the reduction of relaxation time at doping.

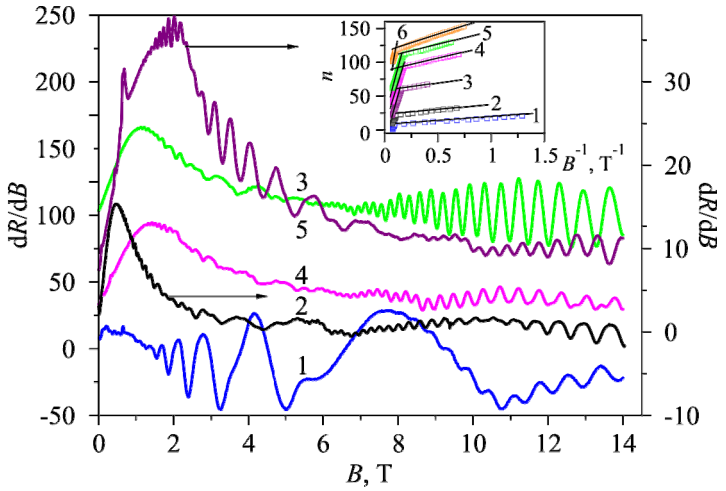

Fig. 3. Field dependences of longitudinal magnetoresistance derivative dR/dB(B) (B || I) at T = 2.1 K of Bi-Sn wires of various composition: 1. Bi – 0.07 at% Sn, d = 0.6 μm; 2. Bi – 0.1 at% Sn, d = 1.5 μm; 3. Bi – 0.15 at% Sn, d = 0.4 μm; 4. Bi – 0.2 at% Sn, d = 0.2 μm; 5. Bi – 0.3at% Sn, d = 1.7 μm. Insert: Dependences of conventional quantum number n of maxima and minima of SdH oscillations of longitudinal magnetoresistance on reverse magnetic field n(B^{-1}).

Insert in Fig. 3 illustrates the dependences of periods of SdH oscillations $\Delta_1(B^{-1})$ and $\Delta_2(B^{-1})$ due to *T*- and $L_{2,3}$-holes, calculated from the linear dependences of quantum number *n* of SdH oscillations due to inverse field $n(B^{-1})$ at different concentrations of *Sn* (in at%).

Period of SdH oscillations due to *T* holes is changed practically by an order from the value $\Delta(B^{-1}) = 0.58 \cdot 10^{-5}$ Oe^{-1} for pure *Bi* to the value $0.055 \cdot 10^{-5}$ Oe^{-1} for the composition *Bi* – 0.05 at% *Sn*. As a result of further increase of *Sn* impurity to 0.3 at%, the period of SdH oscillations is smoothly reduced to $0.032 \cdot 10^{-5}$ Oe^{-1} for the wire *Bi* – 0.3 at% *Sn*.

Similar investigations of the field dependences of the transverse magnetoresistance and SdH oscillations of the wires of all compositions under study were performed in perpendicular magnetic fields when $B \parallel C_2$ ($B \perp I$) and $B \parallel C_3$ ($B \perp I$) (Fig. 4).

In a transverse magnetic field at $B \parallel C_2$ in weak magnetic fields there is a quadratic resistance increase passing to saturation in strong magnetic fields on *R*(*B*) in weakly doped *Bi* wires and to a linear resistance increase in heavily doped *Bi* wires (curves 4, 5, 6 Fig. 4). Maximum resistance increase by 140 – 150 % in magnetic fields up to 14 T occurs in the wires of alloys *Bi* – 0.15 at% *Sn* – *Bi* – 0.2 at% *Sn* (curves 4, 5) which is decelerated at further doping to 0.3 at% *Sn* (curve 6).

In high magnetic fields there are oscillations due to maximum section of *T* holes. With increase in the concentration of *Sn*, the area of existence of SdH oscillations is drastically shifted towards to area of high magnetic fields, reflecting the fact of concentration growth of *T* holes. And for the compositions > 0.1 at% *Sn* the magnetic fields up to 14 T are insufficient to detect SdH oscillations due to maximum section of *T* holes, the area of their existence is shifted to magnetic fields > 14 *T*.

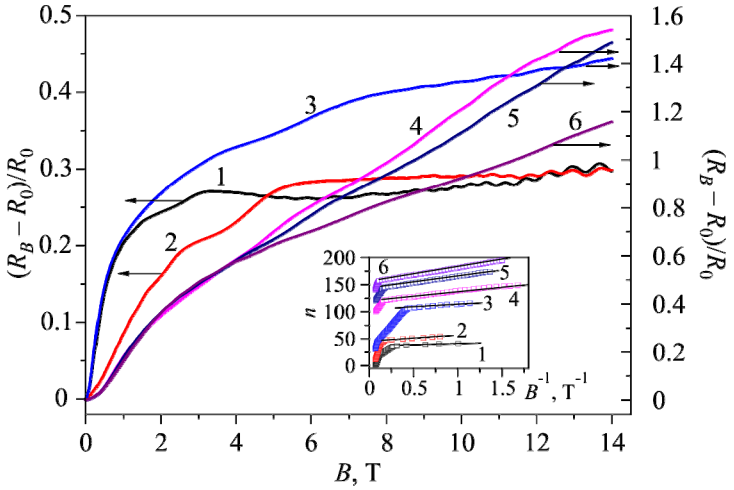

Fig. 4. Field dependences of reduced transverse magnetoresistance ΔR/R(B) (B || C_2) at T = 2.1 K of Bi-Sn wires of various composition: 1. Bi – 0.05 at% Sn, d = 0.6 μm; 2. Bi – 0.07 at% Sn, d = 0.6 μm; 3. Bi – 0.1 at% Sn, d = 1.5 μm; 4. Bi – 0.15 at% Sn, d = 0.4 μm; 5. Bi – 0.2 at% Sn, d = 0.2 μm; 6. Bi – 0.3 at% Sn, d = 1.7 μm. Insert: Dependences of conventional quantum number n of maxima and minima of SdH oscillations on reverse magnetic field n(B^{-1}).

In this direction one can easily see SdH oscillations due to maximum section of L_1-holes and average sections of $L_{2,3}$-hole ellipsoids located symmetrically with respect to a magnetic field $B \parallel C_2$.

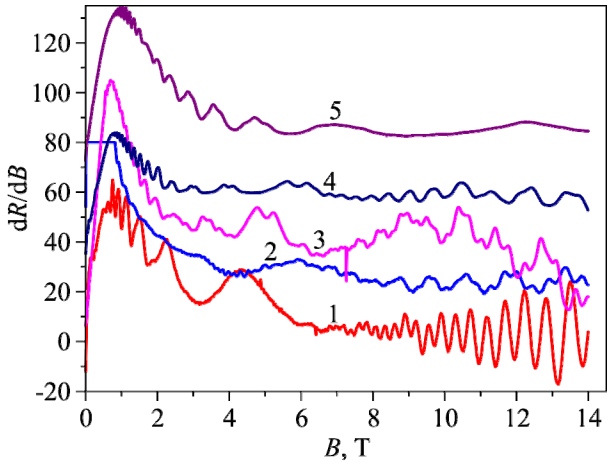

Fig. 5. Field dependences of transverse magnetoresistance derivative dR/dB(B) (B || C_2) at T = 2.1 K of Bi-Sn wires of various composition: 1. Bi – 0.07 at% Sn, d = 0.6 μm; 2. Bi – 0.1 at% Sn, d = 1.5 μm; 3. Bi – 0.15 at% Sn, d = 0.4 μm; 4. Bi – 0.2 at% Sn, d = 0.2 μm; 5. Bi – 0.3 at% Sn, d = 1.7 μm.

As for the case of $B \parallel I$, the greatest change in the periods of SdH oscillations due to both from *L*-holes and *T*-holes was observed in the range of concentrations from pure *Bi* to 0.05 at% *Sn*. A change in the period of SdH oscillations due to maximum section of *L*-holes occurs more smoothly.

At $B \parallel C_3$ ($B \perp I$) there were SdH oscillations due to extreme section of the Fermi surface of *T*-holes close to minimum and the section of *L*-holes close to maximum (Fig. 6, 7).

The specific feature of the field dependences of transverse magnetoresistance at $B \parallel C_3$ at 4.2 K is a drastic quadratic growth of resistance in weak magnetic fields and a transition to linear dependence in high fields. With increase in *Sn* concentration, the area of linear growth of resistance *R*(*B*) is shifted to the area of weaker magnetic fields (curves 3, 4, 5 Fig. 6). As in the case of $B \parallel C_2$, maximum growth of *R*(*B*) was observed in *Bi* wires with the concentration 0.15 – 0.2 at% *Sn*.

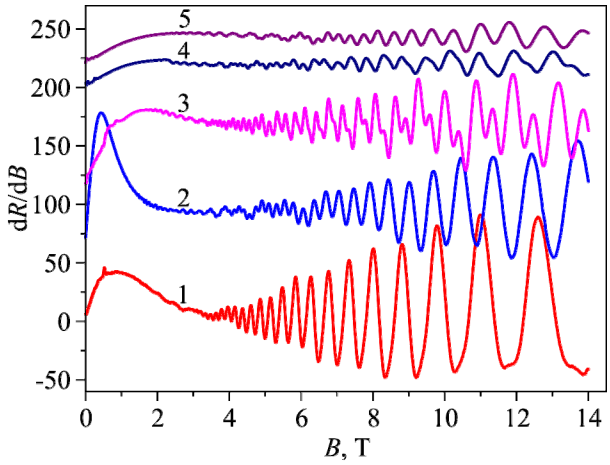

Fig. 6. Field dependences of reduced transverse magnetoresistance ΔR/R(B) (B || C_3) at T = 2.1 K of Bi-Sn wires of various composition: 1. Bi – 0.05 at% Sn, d = 0.6 μm; 2. Bi – 0.07 at% Sn, d = 0.6 μm; 3. Bi – 0.1 at% Sn, d = 1.5 μm; 4. Bi – 0.15 at% Sn, d = 0.4 μm; 5. Bi – 0.2 at% Sn, d = 0.2 μm; 6. Bi – 0.3 at% Sn, d = 1.7 μm. Insert: Dependences of conventional quantum number n of maxima and minima of SdH oscillations on reverse magnetic field n(B^{-1}).

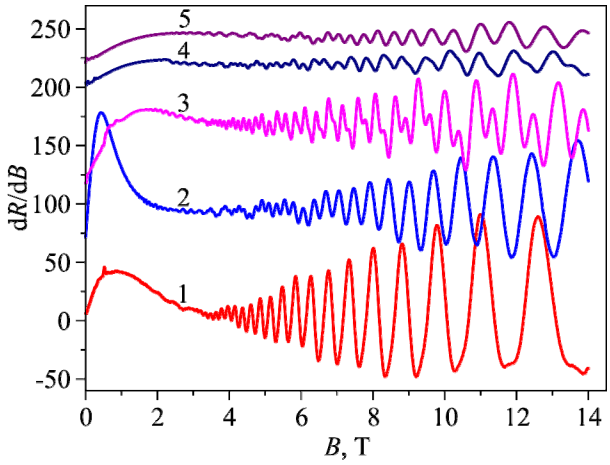

Fig. 7. Field dependences of transverse magnetoresistance derivative dR/dB(B) (B || C_3) at T = 2.1 K of Bi-Sn wires of various composition: 1. Bi – 0.07 at% Sn, d = 0.6 μm; 2. Bi – 0.1 at% Sn, d = 1.5 μm; 3. Bi – 0.15 at% Sn, d = 0.4 μm; 4. Bi – 0.2 at% Sn, d = 0.2 μm; 5. Bi – 0.3 at% Sn, d = 1.7 μm.

Increase in *Sn* concentration to 0.3 at% results in the reduction of periods of SdH oscillations by a factor of 4 – 5.

A combination of investigations of SdH oscillations in *Sn* doped wires in principal crystallographic directions at temperatures 4.2 – 2.1 K allowed calculating the main parameters of the hole surface at *T* and electron surface at *L* at doping with *Sn* donor impurity of *Bi* wires.

For the investigated wires of alloys $Bi_{1-x}Sn_x$ cyclotron masses of extreme maximum and close to minimum sections of the Fermi surface in *T*, were calculated from the temperature dependence of the amplitude of oscillations *R*(*B*) at $B \parallel C_2$ and $B \parallel C_3$ in magnetic fields far from the field of quantum limit where harmonic composition of oscillations is restricted by the first harmonic.

In the case when final temperature T_2 is twofold the initial temperature T_1: $T_2 = 2T_1$, for the cyclotron mass m_c in the quasi-classical range of magnetic fields the following expression was used:

$$m_c = \frac{e\hbar B}{2\pi^2 k T_1 c} \cdot Arcch \frac{A(T_1, B)}{A(T_2, B)}. \quad (3)$$

At T_D = const, ε_F = const: $A(T_1, B)$ is the amplitude of oscillations in field B at $T = T_1$ [10].

The results of calculation of $(m_c^T)_{\max}$ ($B \parallel C_2$) and $(m_c^T)_{\min}$ ($B \parallel C_3$), as well as of mass m_c of sections close to maximum at point T are given in Table 1.

Table 1

The main parameters of the hole Fermi surface at T and the hole Fermi surface at L of investigated Bi-Sn wires with standard orientation (1011) along wire axis in a parallel magnetic field (B || I)

Composition	d, μm	$R_{300}/R_{4.2}$	η_{Sn}	*T*-holes					*L*-holes			
				$\Delta_1(B^{-1})$, 10^{-5} Oe^{-1}	f_1^T, T	m_c^T / m_0	ε_F^T, meV	p^T, 10^{17} cm^{-3}	$\Delta_2(B^{-1})$, 10^{-5} Oe^{-1}	$f_2^{L_{2,3}}$, T	m_c^L/m_0	p^L, 10^{17} cm^{-3}
Bi – 0.05 at% *Sn*	0.6	4.7	0.85	0.055	181.8	0.195	100	116	1.8	5.5	0.033	7.47
Bi – 0.07 at% *Sn*	0.6	4.14	0.7	0.052	194.1	0.224	103.6	120	1.15	8.7	0.034	14.9
Bi – 0.1 at% *Sn*	1.5	8.8	0.6	0.042	240	0.299	117	160	0.85	11.6	0.054	23.1
Bi – 0.2 at% *Sn*	0.2	6.4	0.4	0.041	243	0.311	122	178	0.42	23.8		67.4
Bi – 0.3 at% *Sn*	1.7	7	0.33	0.036	277	0.336	134	210	0.35	28.5	0.0687	88.3

$\Delta_1(B^{-1})$ and f_1^T is period and frequency of SdH oscillations due to close to maximum section $S^T_{\max}$ of the hole Fermi surface at point T ($B \parallel I$); $\Delta_2(B^{-1})$ and $f_2^{L_{2,3}}$ is period and frequency of SdH oscillations due to two equivalent average sections $S^L_{2,3}$ of the hole Fermi surfaces at point L; m_c^T is close to maximum cyclotron mass of holes at point T; m_c^L is cyclotron mass of charge carriers at point L corresponding to average sections $S^L_{2,3}$ of the Fermi surface; ε_F^T is the Fermi energy of holes at point T, calculated in the two-band approximation at ε_g^T = 200 meV; p^T and p^L is hole carrier concentration at points T and L; η_{Sn} is efficiency factor.

Similar calculations were also performed for holes at point L of the Brillouin zone. In some cases, in particular, in the wires of alloys *Bi* – 0.2 at% *Sn* and *Bi* – 0.3 at% *Sn* at $B \parallel C_3$ due to abnormal temperature dependence of the amplitude of SdH oscillations, we did not manage to calculate the cyclotron masses of holes corresponding to minimum section of the Fermi surface of holes at T.

The Dingle temperature T_D for T-holes, as well for L-holes, was determined from the amplitude ratio of SdH oscillations of two consecutive values B_n and B_{n+1}, whereby there are minima and maxima of magnetoresistance according to expression [4].

The calculated values of T_D made 5 – 7 K and did not show a distinct dependence on the composition in the concentration range > 0.05 at% *Sn*.

It was established that the cyclotron masses of T-holes and L-holes grow with increased doping with *Sn* donor impurity. This fact points to spectrum nonparabolicity of not only L-holes, but also T-holes. A similar effect was observed in the bulk samples of *Bi* on doping with tin to concentrations

corresponding to position of the Fermi level of *T*-holes $\varepsilon^T_F = 90$ meV [10].

The Fermi energy ε^T_F of *T*-holes was calculated by the two-band model (ellipsoidal nonparabolic model) by means of expression [11]:

$$\varepsilon^T_F = \varepsilon_{nap} - \frac{1}{2}\varepsilon^T_g + \left[\varepsilon^2_{nap} + \left(\frac{1}{2}\varepsilon^T_g\right)^2\right]^{1/2} \tag{4}$$

$\varepsilon_{nap} = \dfrac{eh\cdot\Delta_T^{-1}}{2\pi c\cdot m^T_c}$, where ε_{nap} is the energy in the approximation of a parabolic band, $\varepsilon_F{}^T$ is the Fermi energy of *T*-holes counted down from the band ceiling at *T*, $m_c{}^T$ is small cyclotron mass of *T*-holes; $\varepsilon_g{}^T$ is a gap at point *T* of the Brillouin zone which according to [11, 12] is equal to 200 meV; $\Delta_T{}^{-1}$ is the value of reverse period of SdH oscillations from the smallest section of hole ellipsoid at *T* point of the Brillouin zone.

From the calculated values of $\varepsilon_F{}^T$ it follows that on doping of *Bi* wires with tin to 0.3 at%, the position of the Fermi level of holes $\varepsilon_F{}^T$ achieves the value ≈ 134 meV, i.e. practically increased by an order as compared to pure bismuth ($\varepsilon_F{}^T = 12$ meV).

The concentration of *T*-holes was calculated by the experimental data of periods of SdH quantum oscillations using the relation [13]:

$$p^T = \frac{1}{3\pi^2}\left(\frac{2e}{\hbar c}\right)^{3/2}\cdot\left(\frac{1}{\Delta_1\Delta_2\Delta_3}\right)^{1/2} \tag{5}$$

where Δ_1, Δ_2, Δ_3 are periods of SdH oscillations in the three main directions of ellipsoid.
Due to the fact that in the investigation of SdH oscillations at $B \parallel C_3$ there were registered oscillations from sections close to minimum (since wire axis makes an angle ~ 20° with the bisector axis $C_{1/2}$), the value of minimum inverse period of *T*-holes in the wires was determined from the ratio $\left(\Delta_T\right)^{-1}_{\min} = \dfrac{\left(\Delta_T^{-1}\right)^d}{2.5}$, where $\left(\Delta_T^{-1}\right)^d$ is the frequency of Shubnikov oscillations of holes in T wires with orientation (10$\underline{1}$1) along the axis in a longitudinal magnetic field. In so doing, it was taken into account that the anisotropy of hole Fermi surface in *T* makes $\dfrac{S_{\max}}{S_{\min}} = 3.2$, and as was shown by the authors of [11] on the bulk *Bi* samples, it is changed at doping with *Sn* to concentration 10^{19} cm^{-3}.

The concentration of carriers of *L*-holes was calculated from the expression:

$$\frac{p^L_{Bi}}{p^L_{alloy}} = \frac{\left(\Delta_1^{-1}\cdot\Delta_2^{-1}\cdot\Delta_3^{-1}\right)^{1/2}_{Bi}}{\left(\Delta_1^{-1}\cdot\Delta_2^{-1}\cdot\Delta_3^{-1}\right)^{1/2}_{Bi-Sn}} = \left(\frac{\Delta^{-1}_{i\ (Bi)}}{\Delta^{-1}_{i\ (Bi-Sn)}}\right)^{3/2}. \tag{6}$$

using as a reference point the concentration of electrons in bismuth at 4.2 K $p = 3\cdot10^{17}$ cm^{-3}. [13] Here, the nonspecularity of hole and electron spectra at point *L* was disregarded. Such inaccuracy has a slight impact on the value of tin efficiency factor η_{Sn}, since η_{Sn} is largely determined by the concentration of impurity holes in *T* ellipsoid.

It is known that total concentration of holes in multiband alloys is determined by the concentration of doping tin impurity C_{Sn} (at%):

$$\Sigma p_i = N_A\cdot\rho_{BiSn}\cdot C_{Sn}\cdot\frac{\eta}{A_{BiSn}}\cdot 100 \tag{7}$$

where N_A is the Avogadro number, ρ and A is the density and atomic weight of *BiSn* alloy.

Comparison of the concentration of holes found from SdH oscillations and calculated by the concentration of doping impurity C_{Sn} for the wires of corresponding composition allowed to determine the efficiency factor η of tin doped wires under study. Factor η is equal to the ratio between excess concentration of charge carriers created by impurity atoms and total concentration of introduced impurity atoms. It turned out that the efficiency factor of tin in glass-coated $Bi_{1-x}Sn_x$ wires obtained by the Ulitovsky method is reduced with increase in *Sn* concentration from the value 0.85 for the wires *Bi* – 0.05 at% *Sn* to 0.3 for the wires *Bi* – 0.3 at% *Sn* and is much in excess of the value η_{Sn} obtained on the bulk samples of $Bi_{1-x}Sn_x$ of respective composition [14-18]. The latter is apparently related to peculiarities of pulling glass-coated single-crystal wires by the Ulitovsky method. Owing to high rates of wire crystallization from the melt which is maintained at high temperature and intensively agitated by electromagnetic field of high-frequency inductor, *Sn* impurity is uniformly distributed, eliminating the possibility of clusters formation in the bulk of the wire pulled from the melt. Therefore, homogeneous single-crystal wires of $Bi_{1-x}Sn_x$ were obtained to concentration 0.3 at% *Sn*. As was shown in [19], the presence of impurity states in doped *Bi* samples leads to a reduction of efficiency factor with a rise in temperature, and at 4.2 K $\eta \approx 1$ and does not depend on concentration, though in the experiments in the bulk samples $\eta << 1$.

The temperature dependences of relative resistance $R_T/R_{300}(T)$ of tin doped bismuth wires in the temperature range of 4.2 – 300 K are illustrated in Fig. 8. With increase in *Sn* concentration above 0.07 at%, the curves $R(T)$ are smooth and identical up to concentration $2.1 \cdot 10^{19}$ cm^{-3}. At *Sn* concentrations 0.07 at%, the size effect in dependences $R_T/R_{300}(T)$ is manifested in displacement of maximum on $R(T)$ to higher-temperature region.

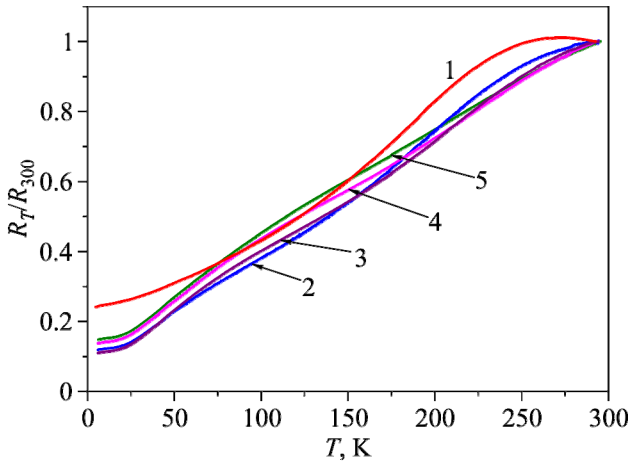

Fig. 8. Temperature dependences of relative resistance $R_T/R_{300}(T)$ of Bi-Sn wires:
1. Bi – 0.07 at% Sn d = 0.3 μm, 2. Bi – 0.1 at% Sn d = 0.9 μm, 3. Bi – 0.15 at% Sn d = 1.1 μm,
4. Bi – 0.2 at% Sn d = 0.6 μm, 5. Bi – 0.3 at% Sn d = 0.9 μm.

The temperature dependences of thermopower α(T) of *Sn* doped bismuth wires are represented in Fig. 9.

For the first time, essential non-monotonous dependence of α(T) with a triple change of thermopower sign in heavily doped alloys (0.1; 0.15; 0.2 at% *Sn*) was discovered. In the alloys with concentration $2.1 \cdot 10^{19}$ cm^{-3} (*Bi* – 0.3 at% *Sn*) the thermopower has positive meaning in the entire temperature range, though curve α(T) is non-monotonous, retaining the peculiarities of curves 2, 3, 4 including change of sign α (Fig. 9).

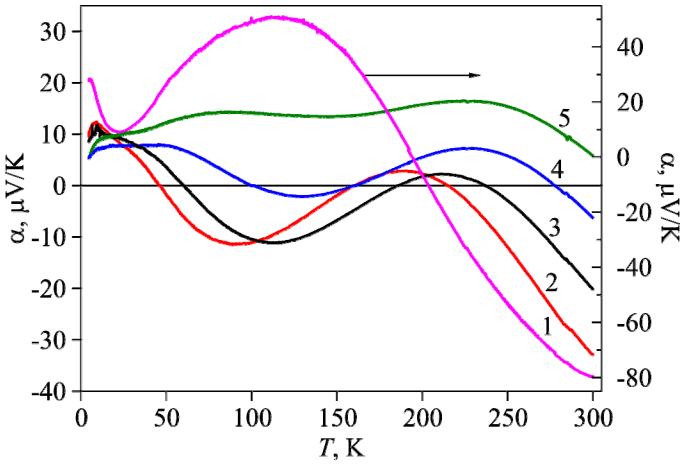

Fig. 9. Temperature dependences of thermopower α(T) of BiSn wires of various composition: 1. Bi – 0.07 at% Sn d = 1.5 μm, 2. Bi – 0.1 at% Sn d = 0.9 μm, 3. Bi – 0.15 at% Sn d = 1.1 μm, 4. Bi – 0.2 at% Sn d = 0.6 μm, 5. Bi – 0.3 at% Sn d = 0.9 μm.

The temperature dependence $\alpha(T)$ for the wires with concentration 0.07 at% *Sn* has a positive maximum in the temperature region 80 – 140 K, following which the thermopower is reduced, remaining in the positive region with temperature reduction to 4.2 K (Fig. 9).

Similar temperature dependences were observed on the bulk samples of $Bi_{1-x}Sn_x$ at concentrations up to 0.26 at% *Sn* [16]. However, on the bulk samples there was no double change of thermopower sign, though the general tendency of thermopower sign change from (–) to (+) with increase in *Sn* concentration took place.

The most interesting effect is a triple change of thermopower sign that was observed in $Bi_{1-x}Sn_x$ wires in the concentration range of $1.6 \div 1.78 \cdot 10^{19}$ cm^{-3} with formation of negative polarity extreme on $\alpha(T)$ in the temperature range of 80 to 100 K. Here it must be emphasized that only holes (light at *L* and heavy at *T*) take part in transition phenomena, and thermopower should be positive. While the first change of sign with temperature reduction from 300 K (in high temperature region) is logical and reflects the fact of intensification of hole contribution to α on doping, the following abnormal change calls for special consideration.

With the contribution to thermopower of two groups of holes: light *L* and heavy *T* or Σ, the total thermopower is determined by the expression:

$$\alpha = \frac{\alpha_L \cdot \sigma_L + \alpha_{T,\Sigma} \cdot \sigma_{T,\Sigma}}{\sigma_L + \sigma_{T,\Sigma}} \qquad (8)$$

where α_L, $\alpha_{T,\Sigma}$, σ_L, $\sigma_{T,\Sigma}$ are partial values of thermopower and electric conductivity of light and heavy holes. The conductivity of heavy *T* or Σ-holes as compared to conductivity of light *L*-holes in the first approximation can be neglected, since mobilities $\mu_{T,\Sigma} << \mu_L$. Therefore, total thermopower for $Bi_{1-x}Sn_x$ alloys is mainly determined by partial thermopower α_L whose value at investigated temperatures is due to operating mechanisms of charge carrier scattering. If hole scattering in *p*-type alloys is only intraband, then, according to theory, the sign of thermopower should be positive.

Thermopower behaviour (change of sign from (+) to (–) and then from (–) to (+) with temperature reduction) allows concluding that thermopower anomaly is related to additional nonintraband scattering mechanism. For light L_S-holes in multi-band alloys such additional scattering mechanism can be elastic scattering of carriers from *L*-band to Σ-band appearing with a displacement of $\varepsilon_F{}^T$ at doping with *Sn*. Further increase in the concentration of impurity holes in the wires of $Bi_{1-x}Sn_x$

alloys leads to anomaly reduction (curve 4), and with heavy doping levels thermopower has a positive meaning and the anomaly disappears (curve 5), which is typical of electron topological transition.

In this case, with electron topological Lifshitz transition $\alpha \sim Z^{-1/2}$, where $Z = (\varepsilon - \varepsilon_k)$ is transition parameter according to theory, thermopower anomaly should be negative, since in the presence of additional scattering channel for the "hot" carriers such as holes in *L* and *T*-bands, thermopower must reduce and can even change sign (negative anomaly).

Thus, electron topological transition occurs when doping *Bi* wires with *Sn* acceptor impurity at concentration $N_c = 1.6 \div 1.8 \cdot 10^{19}$ cm^{-3}, and the estimated energy position of Σ-band corresponds to the Fermi energy value of *T*-holes ε_F^T = 115 to 120 meV.

Note that a similar topological transition with a change of thermopower sign on $\alpha(T)$ was observed in $Bi_{1-x}Sb_x$ alloys doped with *Sn* impurity [12, 20, 21]. The authors also treated this effect from the standpoint of electron topological transition with the origin of Σ-band.

Conclusions

Integrated research of SdH oscillations in the main crystallographic directions of the electrical and thermoelectric properties of single-crystal glass-coated bismuth wires doped with *Sn* acceptor impurity in the temperature range of 1.5 to 300 K is performed. The $\alpha(T)$ dependences are essentially non-monotonous with a triple change of sign in the temperature range of 4.2 – 300 K. Effect of formation of a negative polarity extremum and a double change of sign on $\alpha(T)$ at lower than 200 K temperatures in *Bi-Sn* wires is treated in terms of impurity electron topological Lifshitz transition with heavy doping of bismuth wires with tin. Calculations of the basic parameters of the Fermi surfaces at points *L* and *T* of the Brillouin zone from SdH oscillations allowed estimating the concentration $N_p = 1.6 \div 1.8 \cdot 10^{19}$ cm^{-3} and the energy position of Σ-band ε_F^T = 115 – 120 meV.

This work was performed with support of grant Moldova-Belarus 13.820.05.12/BF.

References

1. I.M. Lifshitz, On the Anomalies of Electronic Characteristics of Metals in the Area of High Pressures, *JETF* **38** (5), 1569 – 1576 (1960).
2. V.G. Vaks, A.V. Trefilov, and S.V. Fomichev, On the Peculiarities of Electric Resistance and Thermopower of Metals with 2 ½ Order Phase Transitions, *JETF* **80** (4), 1613 – 1621 (1981).
3. A.A. Abrikosov, A.V. Pantsulaya, On the Peculiarities of Thermopower with the Lifshits Topological Transition, *Physics of the Solid State* **28** (7), 2140 – 2144 (1986).
4. E.M. Lifshits, L.P. Pitayevsky, *Physical Kinetics* (Moscow: Nauka, 1979), 527 p.
5. A.A. Varlamov, A.V. Pantsulaya, Gigant Thermoelectric Power in Metals in the Vicinity of 2 1*2 Order Phase Transition, *Solid State Communications* **56** (9), 787 – 790 (1985).
6. N.B. Brandt, V.S. Yegorov, M.Yu. Lavreniuk, N.Ya. Minina, and A.M. Savin, Peculiarities of Thermopower and Resistance with Electronic Topological Transitions in Bismuth and its Alloys, *JETF* 89, **6** (12), 2257 – 2269 (1985).
7. D. Gitsu, L. Konopko, A. Nikolaeva, and T. Huber, Pressure Dependent Thermopower of Individual Bi Nanowires, *Applied Physics Letters* **86**, 10210 (2005).
8. A.A. Nikolaeva, L.A. Konopko, A.K. Tsurkan, and T.E. Huber, Thermoelectric Properties of Single-Crystal *Bi-Sn* Wires with Different Crystallographic Orientation at Elastic Strains, *J. Thermoelectricity* **3**, 41 – 59 (2009).

9. N.B. Brandt, D.V. Gitsu, A.A. Nikolaeva, and Ya.G. Ponomarev, Investigation of Size Effects of Thin Cylindrical Bismuth Single Crystals Located in a Magnetic Field, *JETF* **72** (6), 2332 – 2344 (1977).
10. N.B. Brandt, S.M. Chudinov, *Experimental Methods of Research on the Energy Spectra of Electrons and Phonons in Metals* (Moscow: Moscow University Publ., 1983), 408 p.
11. N.B. Brandt, R. Muller, and Ya.G. Ponomarev, Study of the Law of Carriers Dispersion in Bismuth Doped with Acceptor-Type Impurities, *JETF* **71**, 6 (12), 2268 – 2277 (1976).
12. N.A. Redko, N.A. Rodionov, *Letters to JETF* **42** (6), 246 (1985).
13. V.S. Edelman, Properties of Electrons in Bi, *Advances in Physical Sciences* **123**, 257 – 281 (1977).
14. J. Heremans, O.P. Hansen, Temperature Dependence of Excess Carrier Density and Thermopower in Tin-Doped Bismuth. Pseudo-Parabolic Model, *J. Phys. C: Solid State Phys*. **16**, 4623 – 4636 (1983).
15. P.P. Bodiul, A.S. Fedorko, and D.V. Gitsu, Thermo- and Magnetothermoemf in *Bi-Sn* Alloys, *Phys. Stat. Sol.* **1a** (2), p. K77 – K80 (1970).
16. J. Boxus, J. Heremans, J.-P. Michenaud, and J.-P. Issi, The Low-Temperature Thermoelectric Properties of Tin-Doped Bismuth, *J. Phys. F: Met. Phys*. **9** (12), 2387 – 2398 (1979).
17. C. Uher, J.L. Opsal, *Phys. Rev. Lett.* 40, 1518 (1978).
18. J.M. Noothoven van Goor, Donors and Acceptors in Bismuth, *Phil. Res. Rep. Suppl*. 4, 91 (1971).
19. V.F. Garabazhiu, On the Theory of the Impurity Structural Transitions in Weakly Degenerate Systems, *Phys. Lett. A* **112** (1, 2), 38 – 39 (1985).
20. N.A. Redko, N.A. Rodionov, Topological Phase Transitions in $Bi_{1-x}Sb_x$ Alloys and Position of Heavy-Hole Band Versus Composition, *Letters to JETF* **42** (6), 246 – 249 (1985).
21. N.A. Redko, V.I. Belitsky, V.V. Kosarev, N.A. Rodionov, and V.I. Polshin, Heavy-Hole Bands and Thermopower Sign in *Bi-Sb* Alloys, *Physics of the Solid State* **28** (12) (1986).
22. O.S. Griaznov, G.A. Ivanov, B.Ya. Moyzhes, V.N. Naumov, V.A. Nemchinsky, N.A. Rodionov, and N.A. Redko, Influence of Interband Scattering Mechanism on the Kinetic Effects in *p*-$Bi_{1-x}Sb_x$, *Physics of the Solid State* **24** (8), 2335 – 2343 (1982).

Submitted 18.06.14